ELSEVIER

Carbohydrate Polymers 52 (2003) 101–110

Carbohydrate Polymers

www.elsevier.com/locate/carbpol

Starch films reinforced with mineral clay

H.-M. Wilhelm[a,*], M.-R. Sierakowski[a], G.P. Souza[b], F. Wypych[c]

[a]*Laboratório de Biopolímeros, Departamento de Química, Universidade Federal do Paraná, P.O. Box 19081, 81531-990 Curitiba, Paraná, Brazil*
[b]*Laboratório Central de Pesquisa e Desenvolvimento, LACTEC, Curitiba, Paraná, Brazil*
[c]*Laboratório de Química do Estado Sólido, Departamento de Química, Universidade Federal do Paraná, P.O. Box 19081, 81531-990 Curitiba, Paraná, Brazil*

Received 27 November 2001; revised 23 April 2002; accepted 28 August 2002

Abstract

A mineral clay was used as filler in order to improve the mechanical properties of glycerol-plasticized Cará starch films. These were characterized by mechanical and dynamic mechanical analysis, X-ray diffraction (XRD), thermogravimetry, infrared spectroscopy, and scanning electron microscopy. Dynamic mechanical analyses showed that the composite films give rise to three relaxation processes, attributable to a transition of the glassy state of the glycerol-rich phase, to water loss including the interlayer water from the clay structure, and to the starch-rich phase. A film obtained with 30% in w/w of clay showed an increase of more than 70% in the Young modulus compared to non-reinforced plasticized starch. Both XRD and infrared spectroscopy showed that glycerol can be intercalated into the clay galleries and that there is a possible conformational change of starch in the plasticized starch/clay composite films. Clay exfoliation occurred in unplasticized starch/clay mixtures.

Keywords: Starch; Clay; Composite

1. Introduction

There is an ever-increasing interest in the utilization of renewable materials. Among natural polymers, starch has been considered as one of the most promising candidates for the future primarily because of an attractive combination of availability, price and performance. Starch consists of the linear α-D-glucan amylose and highly branched amylopectin. Starches in their native forms, are organized into semi-crystalline granules (Hizukuri, Takeda, Usami, & Takase, 1981; Wurzburg, 1986; Zobel & Stephen, 1995).

Several studies have been carried out on starch-based films obtained by melt processing or casting from a solution or gel with addition of a plasticizer (Wurzburg, 1986). The addition of water (Hulleman, Janssen, & Feil, 1998; Lourdin, Coignard, Bizot, & Collona, 1997) or other plasticizers such as sorbitol (Gaudin, Lourdin, Forssell, & Colonna, 2000) and glycerol (Fishman, Coffin, Konstance, & Onwulata, 2000), considerably improves mechanical properties. Even so, starch films have poor mechanical properties when compared to those of synthetic polymers. This is due to their hydrophilic nature and thus their sensitivity to moisture content, a factor that is difficult to control. The effect of both humidity and plasticizer concentration on crystallinity, thermal and mechanical properties is well documented (Butler & Cameron, 2000; Chang, Cheah, & Seow, 2000; Gaudin et al., 2000; Lim, Chang, & Chung, 2001; Lourdin et al., 1997; Moates, Noel, Parker, & Ring, 2001; Standing, Westling, & Gatenholm, 2001). In order to improve mechanical properties and water resistance, starch has been modified (Fringant, Desbrières, & Rinaudo, 1996; Fringat, Rinaudo, Foray, & Bardet, 1998; Morikava & Nishinari, 2000; Wurzburg, 1986), by blending with synthetic (Arvanitoyannis, Biliaderis, Ogawa, & Kawasaki, 1998; Avérous & Fringant, 2001; Avérous, Moro, Dole, & Ringant, 2000; Psomiadou, Arvanitoyannis, Biliaderis, Ogawa, & Kawasaki, 1997; Sem & Bhattacharya, 2000; Sharma et al., 2001) or natural polymers (Arvanitoyannis, Nakayama, & Aiba, 1998; Curvelo, Carvalho, & Agnelli, 2001; Fishman et al., 2000) and by cross-linking (Chatakanonda, Varavinit, & Chinachoti, 2000; Dumoulin, Alex, Szaba, Cartilier, & Mateescu, 1998). Starch can lowering the cost of the finished product compared with synthetics alone as well as providing biodegradable characteristics.

The preparation of composites can also improve the mechanical properties of materials. The introduction of inorganic fillers to a polymer matrix increases its strength

* Corresponding author. Tel.: +55-41-361-3260; fax: +55-41-361-3186.
E-mail address: wilhelm@quimica.ufpr.br (H.-M. Wilhelm).

0144-8617/03/$ - see front matter © 2003 Elsevier Science Ltd. All rights reserved.
PII: S0144-8617(02)00239-4

and stiffness and sometimes creates special properties, originating from the synergetic effect between the component materials. Among inorganic compounds, special attention has been paid to clay minerals in the field of nanocomposites because of their small particle size and intercalation properties (Alexandre & Dubois, 2000; Kim, Noh, Choi, Lee, & Jhon, 2000; Murray, 2000; Ogata, Kawakage, & Ogihara, 1997).

Mineral clays are technologically important and are mainly composed of hydrated aluminosilicate with neutral or negative charged layers (Murray, 2000). A large number of new composites based on synthetic polymer and clay minerals, have been recently investigated (Chen, Tien, & Wei, 2000; Fornes, Yoon, Keskkula, & Paul, 2001; Liu & Wu, 2001; Magaraphan, Lilayurthalert, Sirivat, & Schwank, 2001; Wu, Xue, Qi, & Wang, 2000). Few studies are reported on biopolymer/clay composites, although, hydroxyapatite-reinforced starch/ethylene–vinyl alcohol copolymer (Reis, Cunha, Allan, & Bevis, 1997) and calcined kaolin/thermoplastic starch composites (Carvalho, Curvelo, & Agnelli, 2001), have been documented. An increase of 50% in the modulus for starch/calcined kaolin composite containing 50 phr (parts of calcined kaolin per hundred parts of thermoplastic starch) of kaolin when compared with a sample prepared without calcined kaolin, was observed (Carvalho et al., 2001).

The optimal performance of polymer/clay composites is achieved when the clay fillers are uniformly dispersed in the polymer matrix.

In the present investigation, Ca^{++}—hectorite (SHCa-1) was added to glycerol-plasticized starch and from this mixture plasticized starch/clay composite films were obtained. The dispersion of clay into the starch matrix and the effect of its addition on the mechanical, thermal, dynamic mechanical properties and morphology of starch/clay composite films, was studied.

2. Materials and methods

2.1. Materials

Native starch, extracted from Cará roots, a Brazilian species, was provided by Universidade Estadual de Londrina (UEL), Paraná. Reagent grade glycerol, and analytical grade K_2CO_3 were used. Ca^{++}—hectorite was supplied by the Clay Mineral Society Repository (University of Missouri, USA). This clay mineral has exchangeable calcium ions, a cation exchange capacity of ~43.9 meq/100 g and a surface area of 63.19 ± 0.5 m^2/g.

2.2. Preparation of plasticized starch/clay composite films

Glycerol-plasticized starch/clay composite films were prepared from starch/clay aqueous suspensions (30 ml) by casting. The starch/clay rations were 100/0, 95/05, 90/10, 85/15, 80/20, and 70/30 (w/w), relative to dry starch, with a total mass of 1.3 g. The clay was dispersed in distilled water (10 ml) for 24 h, producing a gel that was added to an aqueous dispersion of starch (20 ml). This suspension was degassed and heated to boiling point for 30 min with continuous stirring to gelatinize the starch granules. Glycerol (20% w/w, relative to starch on dry basis) was added to the hot solution and the solution was then poured on to polypropylene dishes and solvent evaporated to dryness at 40–50 °C. The films (about 0.15 mm thick) were maintained for 3 weeks at a 43% relative humidity (r.h.), over saturated K_2CO_3 solution in a desiccator at room temperature, according to the specifications of ASTM E 104.

2.3. Characterization of plasticized starch/clay composite films

Portions of the conditioned films were dried at 110 °C for 12 h. After weighting, they were conditioned at 25 °C in a desiccator at 43% r.h., then removed at specific time intervals and weighted. The differences between the initial and final masses correspond to the water loss, thus determining the amount of moisture retained by the films.

X-ray diffraction (XRD) experiments were performed on tape-glued films oriented on neutral glass sample holders. A Rigaku diffractometer operating at 40 kV and 20 mA in the Bragg-Brentano θ–2θ mode was used. A Ni filter as well a graphite monochromator was used to select the correct Co Kα = 1.7902 Å line. Silicon powder was used as the internal standard.

Dynamic mechanical analyses (DMA) of the films were performed using a Netzsch equipment (DMA 242). DMA curves were recorded at temperatures ranging from − 150 to 200 °C heating, with a scanning rate of 2 °C/min. The static force was maintained constant during the experiment. Analyses were performed at frequencies of 1 and 5 Hz. Samples with dimensions of $50 \times 0.5 \times 0.15$ mm^3 were examined.

Thermogravimetric analysis was performed using a Netzsch equipment (TG 209) at a heating rate of 10 °C/min from room temperature to 900 °C, under a synthetic air atmosphere in aluminum crucibles.

Infrared spectra were recorded using a Bomen Michelson FTIR (MB_{100}) apparatus. Transmittance spectra of thin films dried at 100 °C for 24 h, in order to remove water, were obtained by accumulation of 32 scans and a 4 cm^{-1} resolution.

The fractured surfaces of the composites were studied on a Philips scanning electron microscope (XL 30) operating with an accelerating voltage of 10 kV. The fractures were produced by samples frozen in liquid nitrogen. The samples were then sputtering coated with a thin gold film (nominal layer of 250 Å) to avoid charge built up because of their low conductivity.

Tensile testing was carried out using an Instron (4467) tensile testing equipment and cross-head speed of 1.2 mm/min according to the procedures outlined in ASTM D 882. Before testing, the films were allowed to rest for 2 weeks in a 43% r.h. controlled atmosphere, in order to obtain reproducible results. For each data point, five samples were tested, and the average value was taken.

3. Results and discussion

3.1. Dynamic mechanical analysis

Fig. 1 shows the variation of the loss modulus (E'') with temperature for Cará starch with and without glycerol addition.

An unplasticized Cará starch film exhibited two relaxations at the vicinity of −110 °C and at 30 °C. The dominant relaxation that appeared at the lower temperature, is a broad peak relaxation and can be subdivided into two separate components (named λ_1 and λ_2). The λ_1 relaxation can be attributed to rotation of the hydroxymethyl groups and λ_2 to small amplitude oscillations of the sugar rings about the glycosidic bonds. These relaxations have also been observed via dielectric spectroscopy in amylomaize and waxymaize starch with low water contents (Butler & Cameron, 2000). The λ_1 and λ_2 relaxation positions are dependent on frequency. Relaxations that are dependent on the frequency are transitions of the second order, while those that are not, are of the first order. The large α relaxation at a range of ~20–150 °C (Fig. 1(b)), that is frequency independent, is attributable to moisture loss. A measurable glass transition (T_g) was not observed at temperatures of up to 200 °C for the Cará unplasticized starch film, as it should occur at higher temperatures.

The glycerol-plasticized starch films have a different behavior compared to the unplasticized films. The first former gives rise to two dependent frequency relaxations about −74 °C (β_1 relaxation) and 188 °C (β_2 relaxation) (Fig. 1). These can be attributed to two phases that originated from the partial miscibility of glycerol and starch (Forssell, Mikkilä, Moates, & Parker, 1997; Moates et al., 2001): β_1, to a glycerol-rich phase (pure glycerol has a glass transition of −78 °C (Standing et al., 2001) and β_2 to an amylose-rich phase. The appearance of β_2 in the plasticized starch film can be explained by the plastificant effect of glycerol that shifted it to a lower temperature relative to that of unplasticized starch. The α relaxation is decomposed into several small secondary relaxations in the approximate range of 20–150 °C (Fig. 1(b)).

The dynamic mechanical properties of the plasticized starch/clay composite films against composition and temperature are shown in Figs. 2 and 3. The β_1 relaxation values for the various films at 1 and 5 Hz, taken from the maximum of loss modulus curves (E'' curves, Fig. 2(a)) are indicated in Table 1. The position of this relaxation is constant for all the films, with the exception of 90/10 films that present a shift to a higher temperature. The α relaxation of composite films gives a maximum followed by an accentuated shoulder (Fig. 2(b)). We had previously attributed this to moisture loss, but as the shoulder increased significantly after clay addition, this relaxation can also be associated with the crystalline structure of the clay releasing interlayer water molecules. The position of the maximum is dependent on composition, being shifted to higher temperatures with increasing of clay content (Table 1). The formation of H-bonding between the water

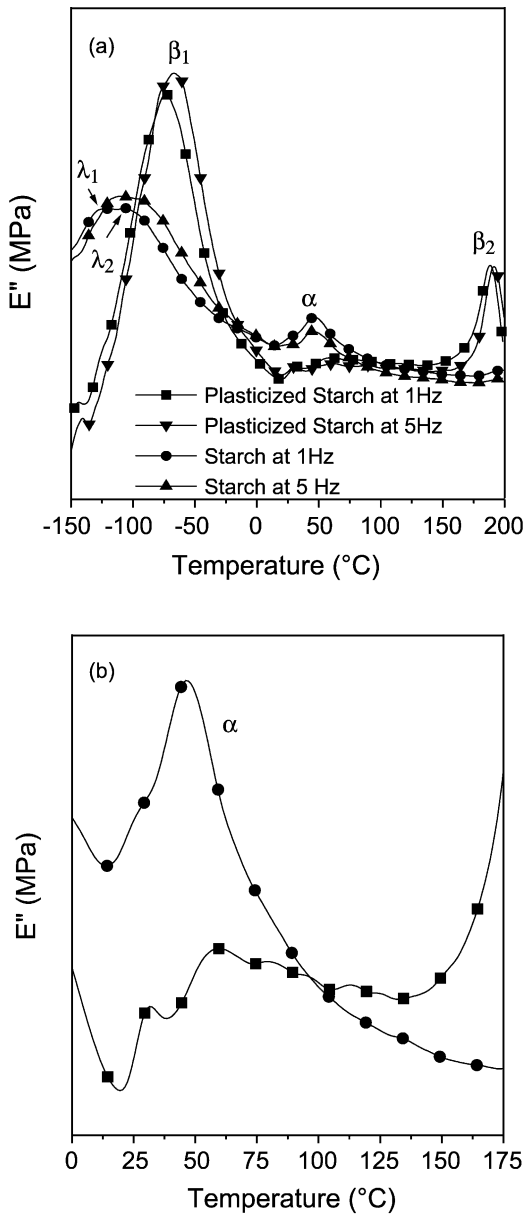

Fig. 1. Loss modulus versus temperature: (a) at 1 Hz, for (●) Cará starch and (■) glycerol-plasticized Cará starch films and at 5 Hz, for (▲) starch and (▼) glycerol-plasticized starch films and (b) at 1 Hz, for (●) starch and (■) glycerol-plasticized starch films from 0 to 175 °C.

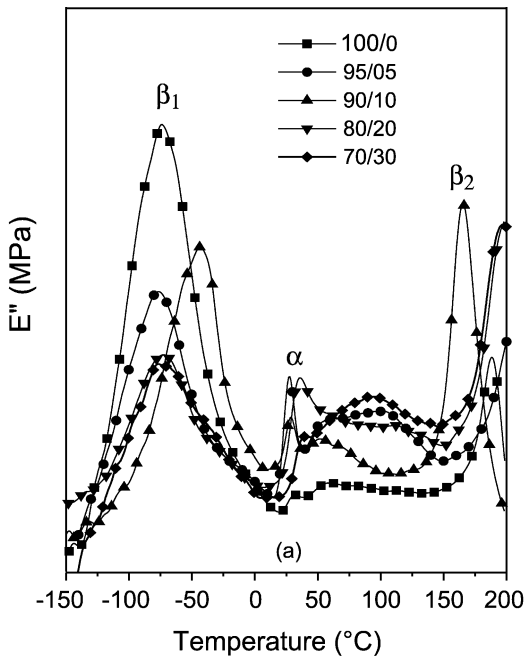

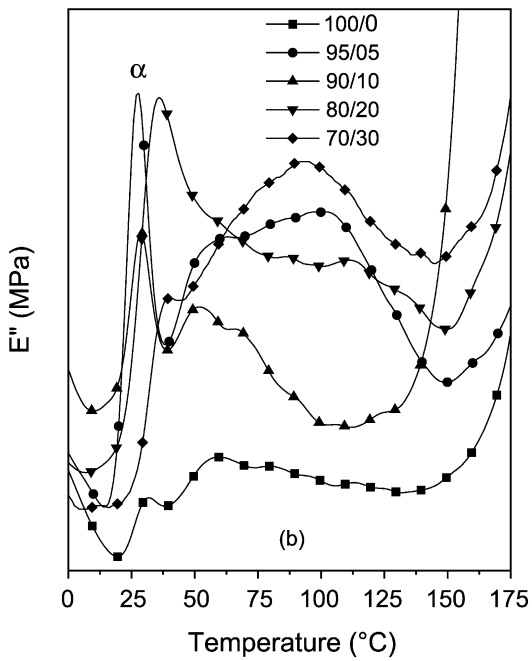

Fig. 2. (a) Loss modulus versus temperature from −150 to 200 °C and (b) loss modulus versus temperature from 0 to 175 °C for glycerol-plasticized Cará starch and Cará starch/clay composite films having different w/w compositions: (■) 100/0, (●) 95/05, (▲) 90/10, (▼) 80/20, and (◆) 70/30.

and the hydroxyl groups of clay or starch in a major extension of the composite films, can explain this α shift.

The exact temperature of β_2 relaxation (relaxation attributed to the starch-rich phase) for the composite films could not be determined under our experimental conditions, because the upper temperature limit was fixed at 200 °C for all films (Fig. 2(a)). Consequently, we determined the onset temperature of this relaxation from the storage modulus

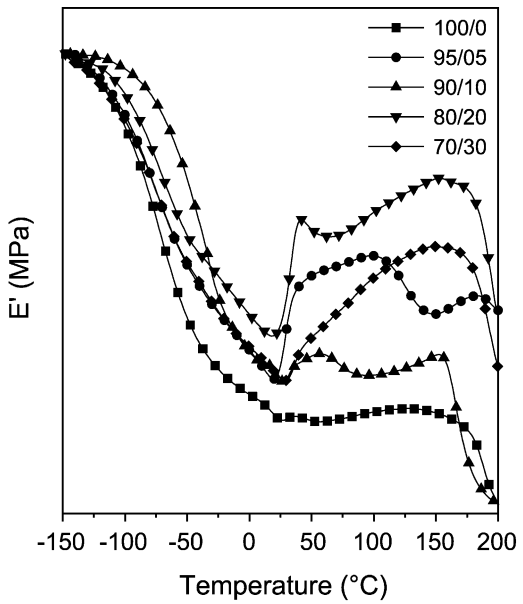

Fig. 3. Storage modulus versus temperature from −150 to 200 °C, for glycerol-plasticized Cará starch/clay composite films having different w/w compositions: (■) 100/0, (●) 95/05, (▲) 90/10, (▼) 80/2, and (◆) 70/30.

curves (E' curves, Fig. 3) and the results obtained are shown in Table 1. The 90/10 film stood out among the others because it presented a considerable shift of β_2 to a lower temperature. The shift of β_1 and β_2 reflects an increase in miscibility between starch and glycerol in the film.

Fig. 2(a) also shows that, on examination of the height of β_1 and β_2 peak relaxations, that β_1 is more intense in plasticized starch, whereas in the composite films β_2 is more intense. To evaluate the effect of the height and to correlate it with the concentration of the respective films, the area of peak E'' for β_1 relaxation was calculated (Table 2). This area can be directly associated with the concentration of segments or groups involved in the relaxation process (Wilhelm, 2000). The area of the composites is smaller than that of the pure plasticized starch film. This was expected due the decrease of the glycerol concentration and the increase of the clay content. Furthermore, if no interaction occurred between starch, glycerol, and clay, the area for β_1 relaxation must be proportional to the glycerol concentration in the films, but this proportionality was not observed. Factors such as intercalation, crystallinity and starch/glycerol miscibility can also contribute to the decrease in area. Assuming that glycerol molecules are intercalated into the clay galleries, their mobility is reduced in function of the clay rigidity; in the same way an increase of crystallinity also leads to lower mobility of the glycerol molecules located in the connecting amorphous regions. A greater glycerol–starch miscibility would reduce the concentration of glycerol on the glycerol-rich phase.

In the same way, if the starch is intercalated into the clay a decrease in the β_2 relaxation would be expected.

Table 1
Temperatures of the relaxation peak for glycerol-plasticized Cará starch and glycerol-plasticized starch/clay composite films at 1 and 5 Hz, as determined by the peak of E'' curves

Composition w/w starch/clay	1 Hz			5 Hz	
	β_1 peak (°C)	α peak (°C)	β_2 peak[a] (°C)	β_1 peak (°C)	α peak (°C)
100/0	−74	32	172	−67	31
95/05	−76	27	180	−71	27
90/10	−43	29	144	−38	29
80/20	−73	36	171	−67	35
70/30	−73	39	169	−67	38

[a] Onset temperatures take from E'' curves.

However, this is not possible since the opposite effect was observed (Fig. 2(a)). In the plasticized starch composite films, the data show that starch is not intercalated into the clay galleries and that does not present any significant increase on crystallinity relative to pure plasticized starch, because as discussed previously both the intercalation and crystallinity restricted the local motions and consequently reduced the area of peak β_2 relaxation.

The increase of the β_2 peak represents an increase in the free starch chain volume, that can originate via a greater plasticization effect, related to the miscibility between starch and glycerol. There is also the possibility that the presence of clay modifies the conformation and orientation of starch chain segments near the surface, giving rise to a β_2 peak increase.

The E' curves (Fig. 3) display an improvement in the storage modulus above 20 °C for composite films, in comparison with pure plasticized starch, and reflects an increase in rigidity, that can originate from film contraction and an increase of crystallinity of the clay filler itself.

To evaluate the hypothesis of film contraction, the change in specimen length during DMA analysis was measured (Fig. 4). When the temperature was raised from −150 to 0 °C, an expansion of all the films occurred, in the order pure plasticized starch > 90/10 > 80/20 > 70/30 films. It is suggested that the lowering of expansion caused by the addition of clay is due to the fine dispersion of silicate layers into the polymer matrices and the filler rigidity. This can obstruct that the expansion of the polymer chains when the temperature is raised.

At ~25 °C, a substantial sample contraction occurred, resulting from the loss of moisture during the heating process, yielding a decrease in the specimen length as the water is lost. This contraction leaves the film more rigid and consequently E' increased for all the films at temperatures >25 °C (Fig. 3). The film with more clay (70/30) presented the lower contraction in comparison with the other samples, indicating more rigidity.

Table 2
Area about $T_{g\ \text{glycerol-rich phase}}$ (β_1 relaxation) determined from E'' curves

Composition w/w starch/clay	β_1 peak relaxation area
100/0	0.53
95/05	0.30
90/10	0.25
80/20	0.16
70/30	0.30

3.2. X-ray diffraction

To evaluate the hypothesis of glycerol and starch intercalation into the clay galleries, XRD analyses were performed. Fig. 5(a) shows the XRD pattern for the clay, glycerol-plasticized starch and respective plasticized starch/clay composite films.

The interplanar basal spacing in pure clay is 14.4 Å. This is shifted with increasing starch content in the composite films, reaching 18.6 Å for 95% starch, showing that glycerol molecules are intercalated between the clay

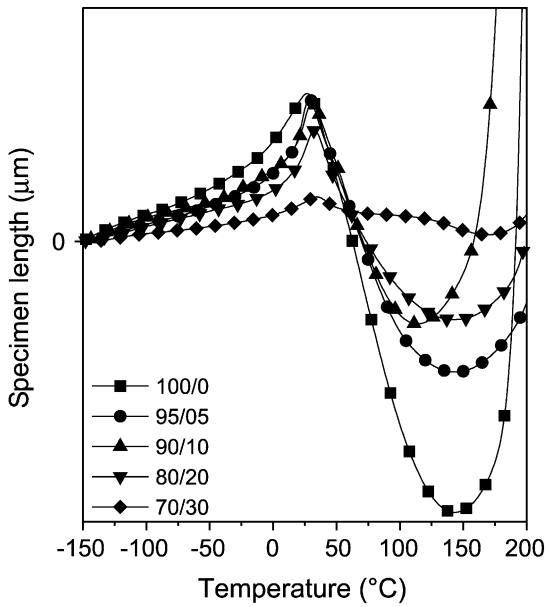

Fig. 4. Specimen length versus temperature for glycerol-plasticized Cará starch and Cará starch/clay composite films having different w/w compositions: (■) 100/0, (●) 95/05, (▲) 90/10, (▼) 80/20, and (◆) 70/30.

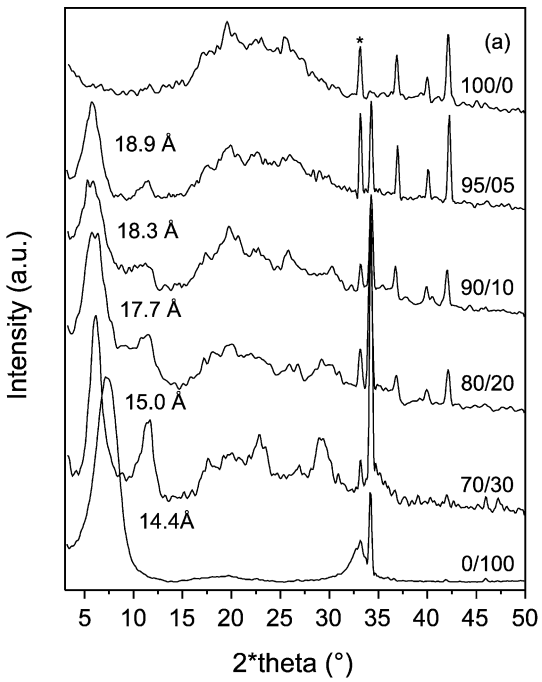

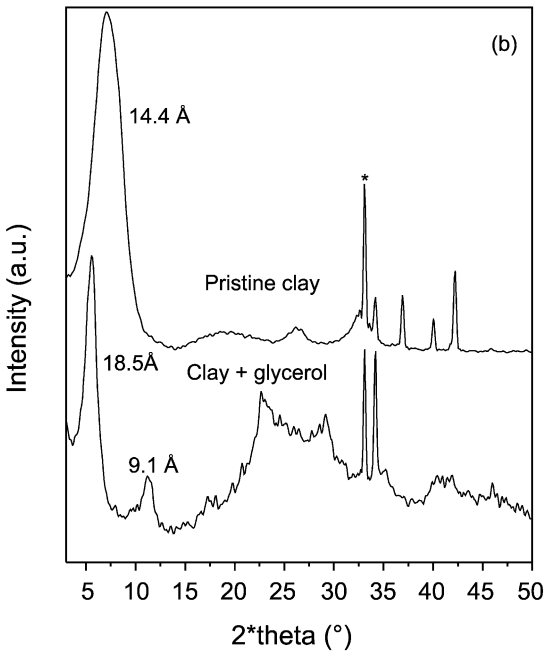

Fig. 5. XRD spectra of (a) glycerol-plasticized Cará starch and Cará starch/clay composite films having different composition and (b) clay/glycerol mixture with an excess of glycerol. Asterisk denotes silicon peak, used as an internal standard.

layers. To investigate the effect of glycerol and starch, we prepared clay/glycerol and unplasticized starch/clay mixtures having different proportions. The interplanar basal spacing in clay/glycerol mixtures was shifted to 18.5 Å (Fig. 5(b)) due to glycerol intercalation between the clay layers.

As in the X-ray diffractograms of 90/10 unplasticized starch/clay mixtures, the first basal peak was not

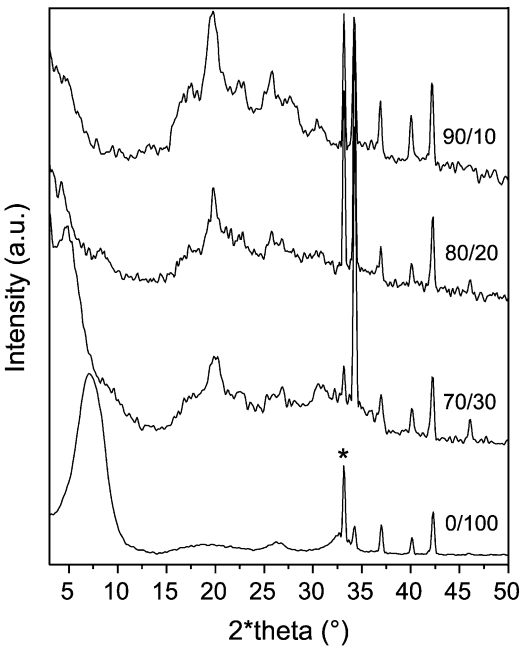

Fig. 6. XRD spectra of unplasticized Cará starch/clay composite films having different compositions.

observed and in this case, the clay can be almost totally exfoliated in the starch matrix (Fig. 6). Although the phenomenon of exfoliation is desirable for the improvement of mechanical properties, the absence of the plasticizer in the starch/clay mixtures increases the brittleness of the samples.

The peak at about 9.3 Å in the composite films can be attributed to dehydrated clay (Fig. 5(a)), corresponding exactly to the loss of two water molecules whose diameter is 5.6 Å. The third peak at a *d*-spacing 3.0 Å is attributed to calcite, a clay impurity (JCPDS, file number: 24–27), and the low *d*-spacing (2.5, 2.6, and 2.8 Å) corresponds to the tape used for film fixation on to the glass sample holder, sometimes observed in the thinner films.

3.3. FTIR analysis

The microdomain structures of the starch and starch/clay composite films were analyzed by FTIR. The main bands for distinctive functional groups were identical in thermoplastic pure starch and pure clay, which makes observation of any modification in these bands difficult (Fig. 7(a)). However, intensity changes in the modes below 800 cm^{-1} were observed, more specifically at 578 and 528 cm^{-1} (Fig. 7(a)). These bands are due to skeletal modes, low frequency vibrations of the ring, etc. (Vasko, Blakwell, & Koening, 1972). The area ratio of these characteristic starch bands is shown in Fig. 7(b) where a decrease of this ratio occurs with an increase of clay content reaching a constant value at a clay content of $\geq 10\%$. These results show that vibration of the glucose

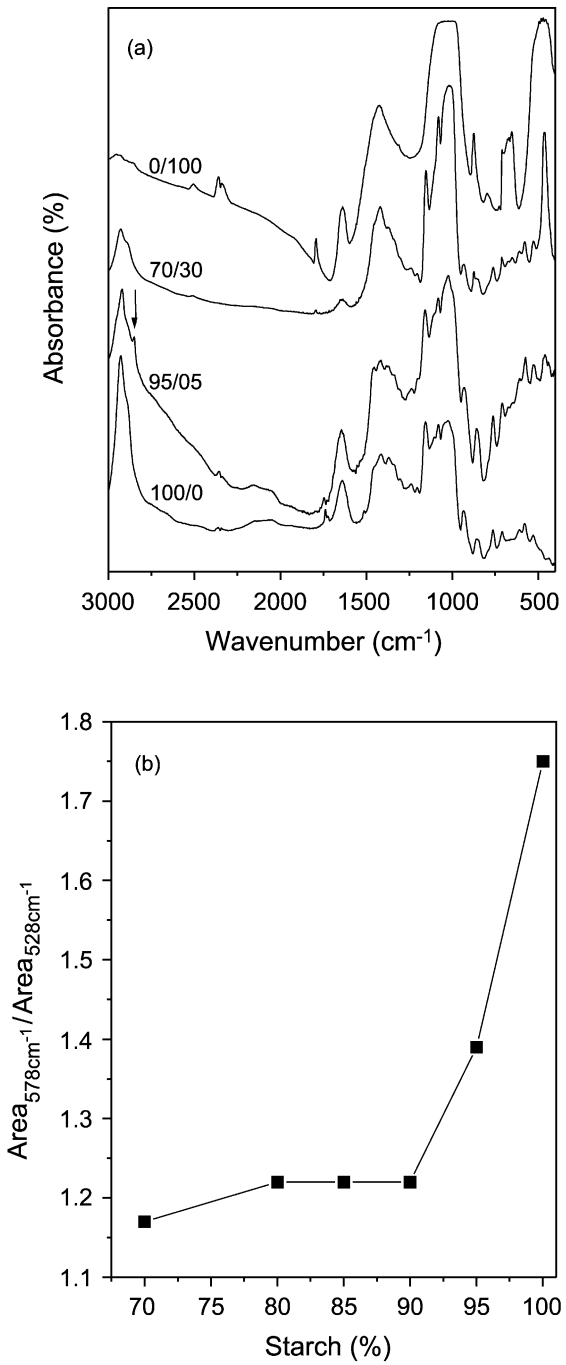

Fig. 7. (a) Absorbance infrared spectra of glycerol-plasticized Cará starch and Cará starch/clay composite films having 100/0, 95/05, 70/30, and 0/100 compositions, at a region from 400 to 3800 cm^{-1}. (b) Area ratio of band at 578 and 528 cm^{-1} for glycerol-plasticized Cará starch and Cará starch/clay composite films versus starch content.

ring is affected by the presence of clay possibly due to conformational changes. The degree of crystallinity will be compared with these results in future studies.

The 95/05 film presents clearer modifications (Fig. 7(a)), such as the appearance of a new band at 2850 cm^{-1}, attributable to CH_2 groups and the increase of intensity of the band at 1463 cm^{-1}, arising from OCH and CH_2 groups (Bellamy, 1998). Pure glycerol presents the first of these bands at 2884 cm^{-1} and the second at 1456 cm^{-1}. These glycerol band shifts confirm that at least a part of the glycerol is located in the clay galleries.

3.4. Thermogravimetric analysis and water sorption

TG analysis results of glycerol-plasticized starch and starch/clay composite films in the temperature range from 19 to 900 °C are shown on Fig. 8. The thermal decomposition of glycerol-plasticized starch followed a three-step reaction with a maximum decomposition at 289 °C. The first step corresponds to the water loss, the second to starch and glycerol decomposition, and the third to the oxidation of the partially decomposed starch. Pure clay shows two degradation steps attributable to water loss (first step) and to clay dehydroxylation at ~725 °C (second step).

The TG curves of starch/clay composite films contain four separate degradation steps. The first three correspond to starch and the last to clay. In general, the presence of clay does not affect the thermal stability of plasticized starch films.

The water loss (Table 3) starts at ~30 °C as determined by the onset. The water absorption of plasticized starch is very high because the water molecules can easily diffuse to H-bonds with OH-groups of glucosyl units along the polymer chains. The starch/clay composite films present very little change on water absorption, in contrast to pure starch (Table 3). The results show that pure plasticized

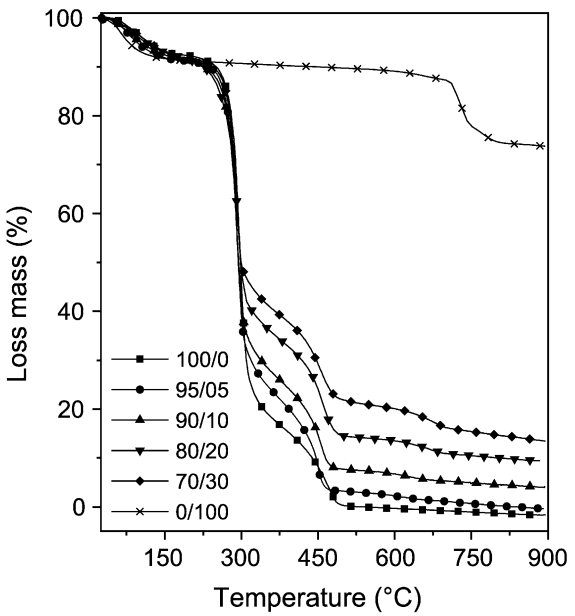

Fig. 8. Thermogravimetric curves for glycerol-plasticized Cará starch and Cará starch/clay composite films having different w/w composition: (■) 100/0, (●) 95/05, (▲) 90/10, (▼) 80/20, (◆) 70/30, and (+) 0/100.

Table 3
Loss of water as determined by the thermogravimetric curves for glycerol-plasticized Cará starch and glycerol-plasticized starch/clay composite films

Composition w/w starch/clay	Loss mass (%)			
	First step	Second step[a]	Third step[b]	Fourth step[c]
100/0	7.9	79.5	20.5	–
95/05	8.9	73.9	26.1	23.0
90/10	8.7	74.9	25.1	23.7
85/15	8.7	73.1	26.9	25.8
80/20	8.6	71.1	28.9	24.7
70/30	8.7	71.9	28.1	26.0
0/100	8.7	–	–	16.4

[a] Mass loss in relation to total mass of the sample.
[b] Mass loss in relation to mass of starch and glycerol in the sample.
[c] Mass loss in relation to mass of clay in the sample.

starch film hydrates in 24 h while the starch/clay composite films takes 36 h for 80/20 mixture.

In plasticized starch, the second and third degradation steps correspond to starch/glycerol and starch degradation, respectively (Fig. 8). The composite films show a larger proportion of mass loss in the third stage, in comparison to pure starch (Table 3). This mass increment can be constituted by glycerol or starch. In the case of glycerol, the intercalated fraction should be protected by the clay being degraded at higher temperatures. In the case of starch, the presence of clay into the glycerol-plasticized starch matrix, induced a re-organized starch structure with less exposed hydroxyl groups, that are less susceptible to degradation, thus contributing to the increase of the mass loss in the third step.

An interesting observation is that the fourth step in the composite films, attributed to clay dehydroxylation, is shifted by ~100 °C to lower temperatures in comparison with pure clay (Fig. 8). Two hypotheses can explain this behavior. Firstly, the third step starch degradation process is an exothermic one, according to Aggarwal and Dollimore (1998) and thus transfers heat to the clay, leading to clay dehydroxylation being shifted to lower temperatures. Secondly, the dispersion of the clay fillers into the plasticized starch matrix promotes an intercalation of the glycerol into the clay galleries, inducing re-organized clay structures, with more exposed hydroxyl groups that are more susceptible to degradation. In pure clay, the mass loss of the fourth step was ~16%, and in the composite films the values are significantly higher (Table 3).

After complete decomposition of the starch (temperature >500 °C), the starch/clay composite film displayed a residue proportional to its clay content (Fig. 8).

3.5. Tensile properties

The tensile properties of glycerol-plasticized starch and starch/clay composite films are shown in Table 4. The pure glycerol-plasticized starch shows an 11% strain at break. This decreases with increasing clay content. A maximum strain break of 5% was found with 30% of added clay. This indicates that adding the inorganic filler into a polymeric matrix increases its brittleness, as shown with another study (Magaraphan et al., 2001).

No significant reinforcing effect was observed up to 20% of clay in the starch matrix, as shown by the Young modulus (Table 4). The increase occurred when the clay content reached 30%, being 72% higher composed with pure non-reinforced starch. These results are better than those reported by Carvalho et al. (2001), who found an increase of 50% in the modulus for glycerol-plasticized starch films reinforced with calcined kaolin obtained using a batch mixer.

3.6. Morphology

The morphology of the glycerol-plasticized starch and starch/clay composite films are shown in Fig. 9. All the starch/clay composite films display an oriented fracture probably, due to the orientation of the crystal clay layered into the starch matrix. This behavior is more pronounced for 80/20 and 70/30 films. Higher magnification was not possible due to degradation of the starch matrix.

Table 4
Tensile strength of glycerol-plasticized Cará starch and glycerol-plasticized starch/clay composite films. The number in parentheses indicate the standard deviation

Composition w/w starch/clay	Young modulus (MPa)	Strain maximum (%)
100/0	815 (90)	11 (3)
90/10	829 (50)	8 (1)
80/20	850 (60)	9 (3)
70/30	1406 (50)	5 (1)

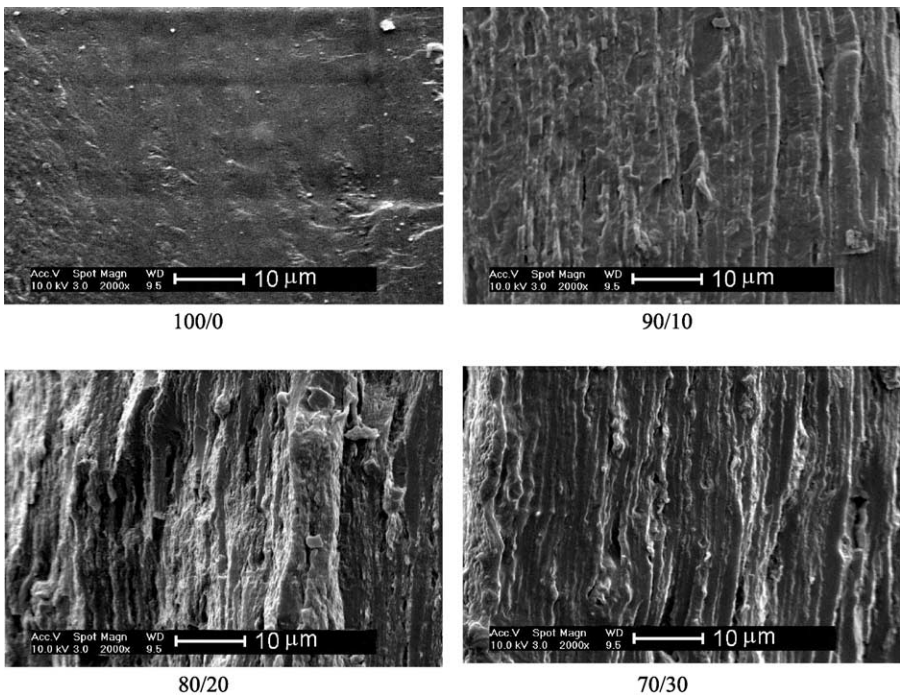

Fig. 9. Morphology of glycerol-plasticized Cará starch and Cará starch/clay composite having different compositions.

4. Conclusion

The structural characterization by infrared spectroscopy and XRD of glycerol-plasticized Cará starch/clay composite films suggest that glycerol is intercalated between the clay layers.

DMA showed that starch and glycerol are partially miscible in such a way that a small fraction of immiscible glycerol exists in all this mixtures, available for the clay intercalation.

The increase of the clay interplanar distance is inversely proportional to the amount of clay amount in the composites and where the clay content is low this distance is identical to the obtained by the glycerol intercalation. Based in this, it can be concluded that intercalation depends on the proportion of available glycerol and clay. On increasing the clay content, a lower ratio was obtained and consequently, the interplanar distance is lowered.

The incorporation of small layered crystals also gave rise to a considerable increase of the storage modulus (stiffness) value at temperatures >25 °C demonstrating the reinforcing effect of the clay on the starch matrix. This was also observed in mechanical tests where the composite film showed better dimensional stability with minimum strain at temperatures from -150 to 200 °C, with an increase of 72% of the Young modulus, on adding 30% clay, when compared to pure plasticized starch.

The above data show that an interaction between glycerol, starch and clay occurs, but to elucidate how this complex system occurs requires further study.

Acknowledgements

Thanks are due to LACTEC, CNPq (Brazilian financing agency), G.-A. Bubniak (for infrared measurements) and to Prof. M.V. Grossman for a gift of Cará starch. Special thanks are due to the personnel of LORXI (Laboratory of the Physics Department UFPR), who made their XRD equipment available.

References

Aggarwal, P., & Dollimore, D. (1998). The effect of chemical starch modification studied using thermal analysis. *Thermochimica Acta*, *324*, 1–8.

Alexandre, M., & Dubois, P. (2000). Polymer-layered silicate nanocomposites: Preparation, properties and uses of a new class of materials. *Materials Science and Engineering R—Reports*, *28*, 1–63.

Arvanitoyannis, I., Biliaderis, C. G., Ogawa, H., & Kawasaki, N. (1998). Biodegradable films made from low density polyethylene (LDPE), rice starch and potato starch for food packaging applications: Part 1. *Carbohydrate Polymers*, *36*, 89–104.

Arvanitoyannis, I., Nakayama, A., & Aiba, S.-I. (1998). Edible films made from hydroxypropyl starch and gelatin and plasticized by polyols and water. *Carbohydrate Polymers*, *36*, 105–119.

Avérous, L., & Fringant, C. (2001). Association between plasticized starch and polyesters: Processing and performance of injected biodegradable systems. *Polymer Engineering Science*, *40*, 727–734.

Avérous, L., Moro, L., Dole, P., & Ringant, C. (2000). Properties of thermoplastic blends; starch–polycaprolactone. *Polymer*, *41*, 4157–4167.

Bellamy, L. J. (1998). *Advances in infrared group frequencies*. Great Britain: Methuen and Co. Ltd.

Butler, M. F., & Cameron, R. E. (2000). A study of the molecular relaxations in solid starch using dielectric spectroscopy. *Carbohydrate Polymers*, *41*, 2249–2263.

Carvalho, A. J. F., Curvelo, A. A. S., & Agnelli, J. A. M. (2001). A first insight on composites of thermoplastic starch and kaolin. *Carbohydrate Polymers*, *45*, 189–194.

Chang, Y. P., Cheah, P. B., & Seow, C. C. J. (2000). Plasticizing–antiplasticizing effects of water on physical properties of tapioca starch films in the glassy state. *Food Science*, *65*, 445–451.

Chatakanonda, P., Varavinit, S., & Chinachoti, P. (2000). Effect of crosslinking on thermal and microscopic transitions of rice starch. *Food Science and Technology*, *33*, 276–284.

Chen, T.-K., Tien, Y.-I., & Wei, K.-H. (2000). Synthesis and characterization of novel segmented polyurethane/clay nanocomposites. *Polymer*, *41*, 1345–1353.

Curvelo, A. A. S., Carvalho, A. J. F., & Agnelli, J. A. M. (2001). Thermoplastic starch-cellulosic fibers composites: Preliminary results. *Carbohydrate Polymers*, *45*, 183–188.

Dumoulin, Y., Alex, S., Szaba, P., Cartilier, L., & Mateescu, M. A. (1998). Cross-linking amylose as matrix for drug controlled release. X-ray and FTIR structural analysis. *Carbohydrate Polymers*, *37*, 361–370.

Fishman, M. L., Coffin, D. R., Konstance, R. P., & Onwulata, C. I. (2000). Extrusion of pectin/starch blends plasticized with glycerol. *Carbohydrate Polymers*, *41*, 317–325.

Fornes, T. D., Yoon, P. J., Keskkula, H., & Paul, D. R. (2001). Nylon 6 nanocomposites: The effect of matrix molecular weight. *Polymer*, *42*, 9929–9940.

Forssell, P. M., Mikkilä, J. M., Moates, G. K., & Parker, R. (1997). Phase and glass transitions behaviour of concentrated barley starch–glycerol mixtures, a model for thermoplastic starch. *Carbohydrate Polymers*, *34*, 275–282.

Fringant, C., Desbrières, J., & Rinaudo, M. (1996). Physical properties of acetylated starch-based materials: Relation with their molecular characteristics. *Polymer*, *37*, 2663–2673.

Fringat, C., Rinaudo, M., Foray, M. F., & Bardet, M. (1998). Preparation of mixed esters of starch or use of an external plasticizer: Two different ways to change the properties of starch acetate films. *Carbohydrate Polymers*, *35*, 97–106.

Gaudin, S., Lourdin, D., Forssell, P. M., & Colonna, P. (2000). Antiplasticization and oxygen permeability of starch–sorbitol films. *Carbohydrate Polymers*, *43*, 33–37.

Hizukuri, S., Takeda, Y., Usami, S., & Takase, Y. (1981). Multi-branched nature of amylose and the action of debranching enzymes. *Carbohydrate Research*, *94*, 205–213.

Hulleman, S. H. D., Janssen, F. H. P., & Feil, H. (1998). The role of water during plasticization of native starches. *Polymer*, *39*, 2043–2048.

Kim, J. W., Noh, M. H., Choi, H. J., Lee, D. C., & Jhon, M. (2000). Synthesis and electrorheological characteristics of SAN-clay composite suspensions. *Polymer*, *41*, 1229–1231.

Lim, S.-T., Chang, E.-H., & Chung, H.-J. (2001). Thermal transitions characteristics of heat-moisture treated corn and potato starches. *Carbohydrate Polymers*, *46*, 107–115.

Liu, X., & Wu, Q. (2001). PP/clay nanocomposites prepared by grafting-melt intercalation. *Polymer*, *42*, 10013–10019.

Lourdin, D., Coignard, L., Bizot, H., & Collona, P. (1997). Influence of equilibrium relative humidity and plasticizer concentration on the water content and glass transition of starch materials. *Polymer*, *38*, 5401–5406.

Magaraphan, R., Lilayurthalert, W., Sirivat, A., & Schwank, J. W. (2001). Preparation, structure, properties and thermal behaviour of rigid-rod polyimide/montmorillonite nanocomposites. *Composites Science and Technology*, *61*, 1253–1264.

Moates, G. K., Noel, T. R., Parker, R., & Ring, S. G. (2001). Dynamic mechanical and dielectric characterisation of amylose–glycerol films. *Carbohydrate Polymers*, *44*, 247–253.

Morikava, K., & Nishinari, K. (2000). Rheological and DSC studies of gelatinization of chemically modified starch treated at various temperatures. *Carbohydrate Polymers*, *43*, 241–247.

Murray, H. H. (2000). Traditional and new applications for kaolin, smectite and polygorskite: A general overview. *Applied Clay Science*, *17*, 207–221.

Ogata, N., Kawakage, S., & Ogihara, T. (1997). Structure and thermal/mechanical properties of poly(ethylene oxide)-clay mineral blends. *Polymer*, *38*, 5115–5118.

Psomiadou, E., Arvanitoyannis, I., Biliaderis, C. G., Ogawa, H., & Kawasaki, N. (1997). Biodegradable films made from low density polyethylene (LDPE), wheat starch and soluble starch for food packaging applications: Part 2. *Carbohydrate Polymers*, *33*, 227–242.

Reis, R. L., Cunha, A. M., Allan, P. S., & Bevis, M. (1997). Structure development and control of injection-molded hydroxylapatite-reinforced starch/EVOH composites. *Journal of Advances Polymer Technology*, *16*, 263–277.

Sem, A., & Bhattacharya, M. (2000). Residual stress and density gradient in injection molded starch/synthetic polymer blends. *Polymer*, *41*, 9177–9190.

Sharma, N., Chang, L. P., Chu, Y. L., Imail, H., Ishiaku, U. S., & Ishaki, Z. A. M. (2001). A study on the effect of pro-oxidant on the thermo-oxidative degradation behaviour of sago starch filled polyethylene. *Polymer Degradation and Stability*, *71*, 381–393.

Standing, M., Westling, A. R., & Gatenholm, P. (2001). Humidity-induced structural transitions in amylose and amylopectin films. *Carbohydrate Polymers*, *45*, 209–217.

Vasko, P. D., Blakwell, J., & Koening, J. L. (1972). Infrared and Raman spectroscopy of carbohydrates. 2. Normal coordinate analysis. *Carbohydrate Research*, *23*, 407–416.

Wilhelm, H. M (2000). *Tese de Doutorado*. Instituto de Química, UNICAMP, Brazil.

Wu, Q., Xue, Z., Qi, Z., & Wang, F. (2000). Synthesis and characterization of PAn/clay nanocomposite with extended chain conformation of polyaniline. *Polymer*, *41*, 2029–2032.

Wurzburg, D. B. (1986). *Modified starches: Properties and uses*. Boca Raton, FL: CRC Press.

Zobel, H. F., & Stephen, A. M. (1995). *Food polysaccharides and their applications*. New York: Marcel Dekker.